


Developing “inverted-corona” fusion targets as high-fluence neutron sources

Cite as: Rev. Sci. Instrum. **92**, 033544 (2021); <https://doi.org/10.1063/5.0040877>

Submitted: 16 December 2020 . Accepted: 06 March 2021 . Published Online: 23 March 2021

 M. Hohenberger,  N. B. Meezan,  W. M. Riedel,  N. Kabadi, C. J. Forrest, L. Aghaian,  M. A. Cappelli,  M. Farrell,  S. H. Glenzer,  B. Heeter, R. Heredia,  O. L. Landen,  A. J. Mackinnon,  R. Petrasso,  C. M. Shulberg, F. Treffert, and W. W. Hsing

COLLECTIONS

Paper published as part of the special topic on [Proceedings of the 23rd Topical Conference on High-Temperature Plasma Diagnostics](#)



View Online



Export Citation



CrossMark

ARTICLES YOU MAY BE INTERESTED IN

[Collective optical Thomson scattering in pulsed-power driven high energy density physics experiments \(invited\)](#)

Review of Scientific Instruments **92**, 033542 (2021); <https://doi.org/10.1063/5.0041118>

[Hot-spot mix in large-scale HDC implosions at NIF](#)

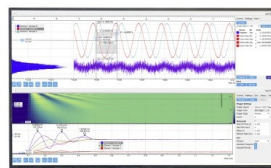
Physics of Plasmas **27**, 092709 (2020); <https://doi.org/10.1063/5.0003779>

[Principal factors in performance of indirect-drive laser fusion experiments](#)

Physics of Plasmas **27**, 112712 (2020); <https://doi.org/10.1063/5.0019191>

Challenge us.

What are your needs for
periodic signal detection?



Zurich
Instruments

Developing “inverted-corona” fusion targets as high-fluence neutron sources

Cite as: Rev. Sci. Instrum. 92, 033544 (2021); doi: 10.1063/5.0040877

Submitted: 16 December 2020 • Accepted: 6 March 2021 •

Published Online: 23 March 2021



View Online



Export Citation



CrossMark

M. Hohenberger,^{1,a)} N. B. Meezan,¹ W. M. Riedel,² N. Kabadi,³ C. J. Forrest,⁴ L. Aghaian,⁵
M. A. Cappelli,² M. Farrell,⁵ S. H. Glenzer,⁶ B. Heeter,¹ R. Heredia,¹ O. L. Landen,¹
A. J. Mackinnon,¹ R. Petrasso,³ C. M. Shulberg,⁵ F. Treffert,^{6,7} and W. W. Hsing¹

AFFILIATIONS

¹Lawrence Livermore National Laboratory, Livermore, California 94550, USA

²Stanford University, Stanford, California 94305, USA

³Plasma Science and Fusion Center, Massachusetts Institute of Technology, Cambridge, Massachusetts 02139, USA

⁴Laboratory for Laser Energetics, University of Rochester, Rochester, New York 14623, USA

⁵General Atomics, 3550 General Atomics Court, San Diego, California 92121, USA

⁶SLAC National Accelerator Laboratory, Menlo Park, California 94309, USA

⁷Institut für Kernphysik, Technische Universität Darmstadt, 64289 Darmstadt, Germany

Note: Paper published as part of the Special Topic on Proceedings of the 23rd Topical Conference on High-Temperature Plasma Diagnostics.

^{a)}Author to whom correspondence should be addressed: hohenberger1@llnl.gov

ABSTRACT

We present experimental studies of inverted-corona targets as neutron sources at the OMEGA Laser Facility and the National Ignition Facility (NIF). Laser beams are directed onto the inner walls of a capsule via laser-entrance holes (LEHs), heating the target interior to fusion conditions. The fusion fuel is provided either as a wall liner, e.g., deuterated plastic (CD), or as a gas fill, e.g., D₂ gas. Such targets are robust to low-mode drive asymmetries, allowing for single-sided laser drive. On OMEGA, 1.8-mm-diameter targets with either a 10- μ m CD liner or up to 2 atm of D₂-gas fill were driven with up to 18 kJ of laser energy in a 1-ns square pulse. Neutron yields of up to 1.5×10^{10} generally followed expected trends with fill pressure or laser energy, although the data imply some mix of the CH wall into the fusion fuel for either design. Comparable performance was observed with single-sided (1x LEH) or double-sided (2x LEH) drive. NIF experiments tested the platform at scaled up dimensions and energies, combining a 15- μ m CD liner and a 3-atm D₂-gas fill in a 4.5-mm diameter target, laser-driven with up to 330 kJ. Neutron yields up to 2.6×10^{12} were measured, exceeding the scaled yield expectation from the OMEGA data. The observed energy scaling on the NIF implies that the neutron production is gas dominated, suggesting a performance boost from using deuterium–tritium (DT) gas. We estimate that neutron yields exceeding 10^{14} should be readily achievable using a modest laser drive of ~ 300 kJ with a DT fill.

Published under license by AIP Publishing. <https://doi.org/10.1063/5.0040877>

I. INTRODUCTION

High-fluence neutron sources are of importance for a wide range of applications in national security and basic science. Examples are active and nonintrusive interrogation,¹ the testing of electronic component vulnerability at high neutron fluxes,² nuclear-cross section and nucleosynthesis studies,³ the irradiation and creation of high-fidelity test samples for forensics exercises,⁴ and neutron radiographic applications.⁵

At the National Ignition Facility (NIF),⁶ high neutron fluxes with integrated yields in excess of 10^{15} neutrons and \sim ns burnwidths are readily achieved with a variety of different experimental inertial-confinement-fusion (ICF) platforms. Common to all of these is the symmetric compression of a deuterium–tritium (DT) fusion-fuel filled capsule to reach temperatures of a few keV, thus initiating D–T fusion reactions and releasing neutrons.^{7–9} The fuel is heated to fusion conditions by coupling laser energy into an ablator material of a low atomic number, typically plastic (CH), beryllium,

or high-density carbon. This is performed either in a direct-drive geometry, with the laser directly incident onto the target, or via a high-Z cavity that converts the laser into x rays incident onto the target located at the cavity's center. Importantly, common to either approach is the necessity for a spherically symmetric drive and thus the requirement for a nearly spherically symmetric laser delivery.

A new approach for a laser-driven neutron-source platform with significantly less-stringent laser-symmetry requirements, but compatible with long-pulse, ICF facilities, was motivated by a recent publication describing experiments on the ShengGuangIII-prototype Laser Facility.¹⁰ In this scheme, laser beams illuminate the inner walls of a hollow target, e.g., a sphere or a cylinder, entering the target through one or more laser-entrance holes (LEHs). The laser heating ablates a layer of fusible material on the inside surface of the target, e.g., deuterated plastic (CD), with the low-density ablative flows converging at the target's center. Eventually, the ablation plasma transitions from long-range interactions to collisional stagnation, thereby heating the ions to fusion conditions through thermalization of the ablative plasma flows. The principle idea was first described in 1987 by Japanese researchers,¹¹ was subsequently coined *inverted-corona fusion*,¹² and has since been investigated by various research groups at the kJ drive level.^{13,14} Notably, Ref. 10 provides a scaling discussion that argues that single-shot neutron yields of order 10^{17} may be feasible using this platform on the NIF with a cryogenic DT layer instead of deuterated plastic and utilizing NIF's full energy capability of 1.8 MJ.

This paper discusses experiments testing the performance scaling of inverted-corona targets to increased laser-drive energies in excess of 100 kJ and the feasibility of this platform for applications on the NIF. This paper is organized as follows: Section II introduces the inverted-corona platform and discusses two target designs, a liner target and a gas-filled capsule. Section III describes experiments performed at the OMEGA Laser Facility and the NIF testing the scaling of its performance with laser energy and fill pressure. Finally, Sec. IV summarizes our results and briefly discusses potential applications.

II. THE INVERTED-CORONA PLATFORM

The principle design of the inverted-corona fusion platform is shown in Fig. 1. Here, the inside volume of a hollow target is heated to fusion conditions via laser heating, with laser beams entering the target through one or more LEHs and incident onto the inside surface. The fusion fuel may be provided in a variety of different ways, two of which are discussed below. In its most simple form, the fusible material is contained within the inner wall itself, e.g., as deuterated plastic (CD), with the target interior volume at vacuum. This is the design discussed in the literature so far. Here, the laser-energy deposition drives a plasma expansion of the inner-wall

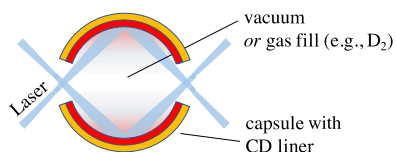


FIG. 1. In the inverted-corona platform, laser beams are pointed onto the inside walls of a capsule via LEHs, thus driving inner-wall ablation and central stagnation and heating the interior to multi-keV temperatures.

surface toward the target center. As the ablative flows converge, the plasma density increases and the ions transition from long-range interactions to collisional stagnation, heating the plasma and generating fusion reactions. The plasma conditions at the target center may be estimated by considering that the leading edge of the ablating plasma can reach velocities of order $10^3 \mu\text{m/ns}$. The stagnation temperature, T_i , of an ion moving at velocity v_i can be calculated via $3kT = m_i v_i^2$, where k is the Boltzmann constant and m_i is the mass of the ion. For a deuterium ion, this gives a temperature of roughly 7 keV, sufficient for fusion reactions.

Following a similar derivation to Ref. 10, but assuming a mass ablation rate of $\dot{m} \sim I_L^{1/3}$, with I_L being the laser intensity, and a reactivity of $\langle \sigma v \rangle_{DD} \sim T^{2.5}$, with T being the ion temperature, one can derive an expected yield scaling for a CD-lined target of

$$Y_{\text{liner}} \sim \left(\frac{E_L}{R} \right)^2, \quad (1)$$

where E_L is the incident laser energy and R is the initial target radius. Alternatively, the fusible material can be provided as a gas fill, such as D_2 or DT gas, inside a low-Z target. In this case, the plasma heating process becomes similar to an exploding pusher.¹⁵ The laser-driven ablation launches a shock into the gas fill, with the expanding wall plasma acting as a piston, thus heating the capsule fill. As the shock converges at the center, the ion temperature and density increase and fusion reactions occur until sufficient cooling and disassembly of the fuel. Similar to Eq. (1), one finds that the yield for gas-filled targets is expected to scale as

$$Y_{\text{gas}} \sim \rho \left(\frac{E_L R}{\tau} \right)^{4/3}, \quad (2)$$

with ρ being the fill-gas mass density and τ being the laser pulse width. Notably, the gas-fill approach results in a more complicated target than the liner target discussed above as the LEHs need to be covered by windows to contain the gas fill. The windows are kept thin, $\sim 1 \mu\text{m}$, to limit their impact on laser propagation, similar to the LEH windows used in ICF *Hohlraum* targets,¹⁶ resulting in significant permeation rates of the gas fill through the windows. Thus, such a target needs to be fielded with a fill tube and a gas reservoir.

For a hydrodynamically scaled system, where scale is defined as the ratio of target radii $S = R_1/R_0$ and pulse width and energy scale are S and S^3 , respectively, either yield formula reduces to the standard performance scaling of $Y \sim S^4$.

III. EXPERIMENTAL DATA

Experiments were conducted at the OMEGA Laser Facility¹⁷ to test the inverted-corona neutron source at the multi-kJ drive level and to explore its potential for high-energy-density (HED) application on the NIF.⁶ The experimental layout is shown schematically in Fig. 2. The targets were manufactured from Glow Discharge Polymer (GDP)¹⁸ with an inner diameter of 1.8 mm and 25- μm thick walls, minimizing outward acceleration of the capsule walls prior to peak neutron emission. Fusion fuel was provided either as a 1- to 2-atm, room-temperature D_2 -gas fill in a CH-wall target or in a vacuum target as a 10- μm deuterated plastic (CD) liner on the inside of the CH wall [see Fig. 2(a)]. The LEHs were aligned along the P5/P8

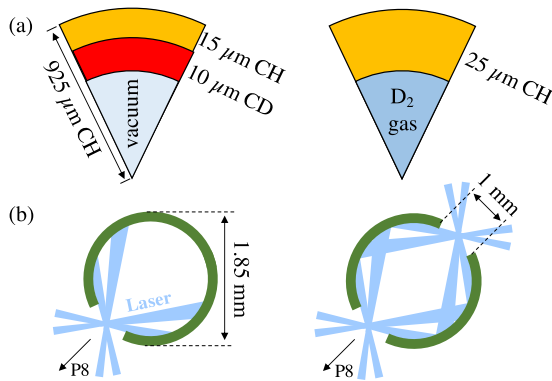


FIG. 2. Schematic configuration of the OMEGA experiments. (a) Fusion fuel was included either as a CD liner in a vacuum target or as a D_2 -gas fill in a CH-only capsule. (b) The laser beams were pointed onto the inside wall through either one or two LEHs oriented along the P5/P8 OMEGA chamber axis.

axis of the OMEGA chamber [see Fig. 2(b)]. Up to 40 beams irradiated the target using 1-ns square pulses, with all beams at nominally the same power, co-timed, and up to 500 J/beam. The 40 beams were pointed evenly onto the inner wall for maximized irradiation uniformity and focused at or near the LEH plane to minimize the required LEH size. A key feature of the inverted-corona platform is its robustness to drive asymmetries, allowing for single-sided laser drive and unique experimental geometries such as pump-probe-type neutron experiments or neutron-radiography applications. To test this, experiments were performed using the 10- μm CD-liner target with both 1x and 2x LEHs and laser-driven at comparable total energies. For the 1-LEH case, half the beams were simply turned off without repointing the remaining beams. All the gas-filled OMEGA targets used 2x LEHs.

The yield obtained with the CD-liner targets is shown in Fig. 3 as the red, solid squares, plotted as a function of the scaling relation in Eq. (1), together with the data reported by Ren *et al.* in Ref. 10. Error bars are on the order of 10% and smaller than the data points in the plot. From left to right, the OMEGA data were obtained with laser energies of 9.1 kJ (1x LEH), 10.3, and 18.5 kJ (2x LEHs), giving neutron yields of 7.0×10^9 , 8.3×10^9 , and 1.5×10^{10} , respectively.

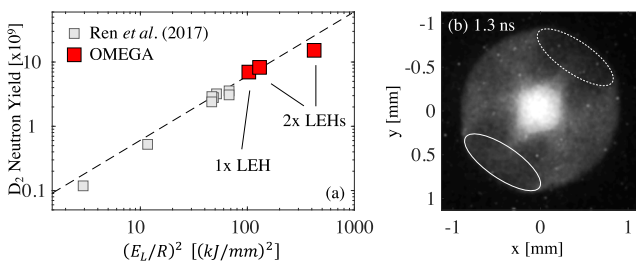


FIG. 3. (a) Neutron yields of the 10- μm CD-liner targets vs the scaling in Eq. (1). Gray squares are reproduced with permission from Ren *et al.*, Phys. Rev. Lett. **118**, 165001 (2017). Copyright 2017 APS. The 1- and 2-LEH data give similar performance at the same drive, while the highest-energy data point is lower than the predicted scaling (dashed line). (b) Framing-camera data at 1.3 ns for a CD-lined target driven with 18.5 kJ. The white lines indicate the LEH positions.

Notably, the performance was robust to significant drive asymmetries. Using Eq. (1) to correct for the laser energy, the two experiments at ~ 10 kJ performed to within 7% of each other and well within the error bars. This is despite the 1-LEH experiment turning off one hemisphere of beams, without introducing any beam repointing. Such low-mode drive asymmetry would introduce a substantial performance impact on conventional, compressively driven neutron sources.

The dashed line in Fig. 3 is a linear fit to all data except for the 18.5-kJ data point to the far right. The yields largely follow the linear trend, consistent with the previously published data. Interestingly, the highest-energy data point is low by $\sim 40\%$ compared to the linear fit, with a predicted yield of $\sim 2.6 \times 10^{10}$. One hypothesis for this deviation is that the expanding wall material undergoes turbulent mixing as it expands inward. This introduces non-fusionable CH-wall material into the ablating CD plasma, quenching the D-D fusion reactions in the central, hot region. Wall ablation and mix should scale with incident laser energy, hence the deviation at the highest drive, implying that a thicker liner or a pure CD wall may increase the yield further.

A second series of OMEGA experiments tested the yield scaling with D_2 -gas fill density in CH-wall targets with 2x LEHs, each covered by 1- μm polyimide foils glued to the outside of the capsule [see Fig. 4(a)]. The capsules were connected to a gas reservoir via a 125- μm diameter, stainless-steel fill tube, which also acted as the target stalk. The room-temperature fills were varied between 1 and 2 atm, with the upper limit set by the window burst pressure. The yield results from the gas-fill scan are shown in Fig. 4(b) plotted against the scaling in Eq. (2), with different pressures represented as different shades of blue and the dashed lines being linear fits through the separate pressure data. Interestingly, the data do not follow a single linear scaling. Indeed, the fitted slope increases with pressure, with the 2-atm data giving an almost 50% steeper slope than the 1-atm data. While further analysis of these data is required, this may also be explained by mix of non-fusionable wall material into the D_2 gas. Similar to the role of the *Hohlraum* gas fill in an indirect-drive ICF target, increasing the fill pressure will suppress wall expansion,¹⁶ thus minimizing the abundance of non-fusionable ions in the central, hot region where the fusion reactions are taking place. An implication of this interpretation is that the slope, and the

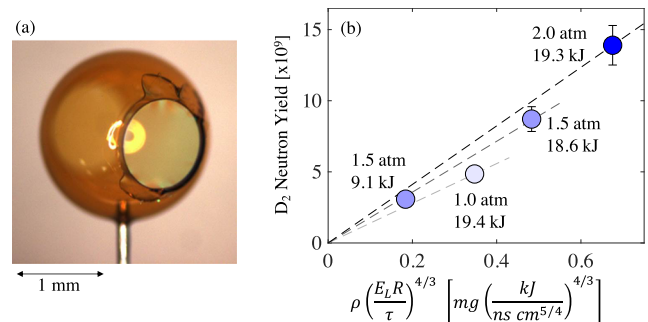


FIG. 4. (a) Photograph of a gas-filled OMEGA capsule. A 1- μm polyimide window is glued to the LEHs to contain the gas fill. (b) Neutron yields vs the scaling in Eq. (2). The data do not follow a single linear scaling, with increased performance at higher pressure than predicted.

yield performance, may increase further with higher pressures, up to a maximum fill where wall expansion is sufficiently tamped.

The experiments did not image the neutron-emitting region directly, but x-ray images, as shown in Fig. 3(b), exhibit an emission region of $\sim 450\ \mu\text{m}$ or 25% of the initial target size. The data shown are for a 2-LEH vacuum target driven with 18.5 kJ, at 1.3 ns, roughly at peak x-ray vacuum as observed by the framing camera, and the data are representative of both gas-filled and vacuum targets. The cameras were sensitive to emission $>1\ \text{keV}$, and the x-ray hot spot can be considered an upper bound of the neutron-emitting region.

Following the proof-of-principle work conducted at OMEGA, experiments tested the platform performance on the NIF with laser drives $>100\ \text{kJ}$. A schematic of the NIF target with a 4.5-mm inner diameter and a $100\text{-}\mu\text{m}$ wall is shown in Fig. 5(a). An interesting application is neutron radiography of a second target driven via a subset of NIF beams. Accordingly, the NIF experiments focused on a single-LEH design, using only the bottom 96 NIF beams to drive the target. To reduce potential yield degradation from CH-wall mixing into the fuel, the target combined a room-temperature, 3-atm D_2 -gas fill with a $15\text{-}\mu\text{m}$ CD liner. A $1\text{-}\mu\text{m}$ -thick polyimide foil covered the 2.5-mm-diameter LEH, and the gas fill was provided via a $70\text{-}\mu\text{m}$ -diameter SiO_2 fill tube. Two experiments were conducted: the first one used a laser drive hydrodynamically scaled from the single-LEH OMEGA experiment (2.5 ns square laser pulse, 140 kJ) and the second one increased the laser energy to 330 kJ with the same pulse shape. The measured yields of 1.3×10^{12} and 2.7×10^{12} are plotted in Fig. 5(b) as a function of laser energy (green diamonds), and the respective ion temperatures were 5.8 and 7 keV. Since the NIF experiments combined both a gas fill and a CD liner for the fusion fuel, a direct comparison with the OMEGA data is difficult. However, it is worth comparing the results to the scaled performance for either design using the appropriate relations [Eqs. (1) and (2)]. This is shown as the red squares and blue circles for the liner and gas-fill data, respectively. The gas-fill yield was scaled using the 2-atm data [Fig. 4(b)], assuming that the higher gas fill minimized a potential impact of yield degradation from mix. The CD-liner data were scaled using the fit (dashed line) in Fig. 3.

A potential concern for the inverted-corona platform as a neutron source is the generation of hot electrons and x rays. The NIF diagnostic FFLEX provides time-resolved measurements of hard

x rays above 18 keV.¹⁹ However, FFLEX is also sensitive to x rays from neutrons scattering inside the NIF chamber, and at neutron yields $> 10^{12}$, this is known to contribute significantly to the signal. Nonetheless, using the FFLEX data to provide an upper limit, the hot-electron population is found to contain $\sim 1.5\%$ of the incident laser energy at a temperature of $\sim 40\ \text{keV}$. This is a higher conversion efficiency than that of direct-drive designs, which typically exhibit an order of 0.5% at comparable laser energies and which is likely caused by the extended laser path through the gas-filled capsule generating stimulated Raman scattering (SRS). However, because of the neutron background in the FFLEX data, these results should be considered an upper limit.

Notably, the NIF experiments outperform the OMEGA-scaled data by factors of a few at both laser energies. In addition, although a fit to the NIF data gives $Y_{\text{NIF}} \sim E_L^{0.9}$, weaker than either scaling in Eqs. (1) and (2), the performance appears to be dominated by the gas fill, rather than the ablation of the CD-liner material. This is a promising result, and higher yields should be readily achievable with a DT gas fill, rather than the much more challenging substitution of the CD liner with DT (e.g., as a cryogenic DT layer or using wetted-foam targets). At the ion temperatures measured on the NIF experiments, $(\sigma v)_{\text{DT}}/(\sigma v)_{\text{DD}} \approx 160$, and yields of $3\text{--}4 \times 10^{14}$ are feasible on the NIF with below-optics-damage laser drives in single-LEH targets. Utilizing all 192 NIF beams and moderate power/beam is expected to give neutron yields in excess of 10^{15} .

IV. CONCLUSIONS AND OUTLOOK

Experiments were performed at OMEGA and the NIF testing the scalability of inverted-corona fusion targets using both CD-lined and gas-filled targets. A number of key conclusions can be drawn from this work. At the 10-kJ drive level, the CD-lined target performance is consistent with previously published data, but a deviation from the expected scaling at higher energy may be attributed to yield degradation from non-fusionable wall material mixing into the central region of the CD-ablator plasma. Robustness to laser-drive asymmetries was demonstrated using 1x and 2x-LEH designs. Gas-filled CH targets with room-temperature D_2 exhibited a stronger dependence on the fill pressure than predicted, also indicating some mix of non-fusionable wall material into the fuel. NIF experiments with $>100\ \text{kJ}$ drives combined both a CD liner and a D_2 fill in the same target, with the resulting D_2 neutron yields $> 10^{12}$ significantly exceeding the scaled performance of both the OMEGA data with either design. Future experiments will explore design variations to access higher yields and investigate the role of mix for these targets. Additionally, both particle-in-cell and hydrodynamic simulations are being developed to better understand the role of kinetic effects on the target evolution during plasma interpenetration and stagnation.²⁰

The inverted-corona fusion platform offers many interesting applications for HED research and basic sciences. In contrast to DT-layered target implosions or traditional, compressively driven platforms, the resulting neutron fluxes are spatially uniform (no fuel areal-density variations), and the spectrum is nearly monoenergetic (no downscattering in the compressed fuel). The target itself is spherical, and samples mounted on the outside of the capsule, e.g., for cross-sectional studies, are not subject to geometrical

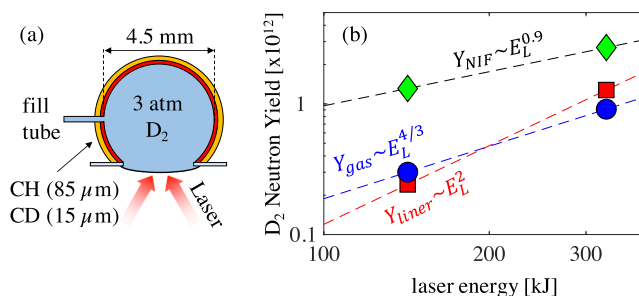


FIG. 5. (a) Schematic of the NIF-scale target combining both a CD liner and a D_2 -gas fill. (b) The NIF-measured performance (green diamonds) exceeds the yield scaled from the OMEGA data for both the CD-liner (red squares) and the gas-fill (blue circles) targets.

flux variations as is the case with cylindrical *Hohlraums*. Including relevant elements in the ablated wall material also allows performing nuclear measurements on nuclei with excited levels in thermal equilibrium, an important complement to experiments at accelerator laboratories where targets are at ambient temperature. Furthermore, the platform is not subject to significant performance penalties from drive asymmetries and can be driven from a single side, thus freeing up laser beams and enabling unique experimental geometries on the NIF. With integrated neutron yields of 10^{15} , neutron fluxes in excess of 10^{23} neutrons/cm²/s are achievable at the target wall, orders of magnitude higher than what is feasible with conventional neutron sources, e.g., reactors or spallation sources. Additionally, there are many conceivable variations of the target designs discussed here, which may improve performance further, albeit at the cost of target complexity. For example, one may consider adding a high-Z enclosure around the target to limit radiative energy losses and the radiative cooling rate of the stagnating plasma. A higher-yield liner-type target could be realized using a wetted-foam design or a cryogenic DT layer, which would require a thermo-mechanical package for temperature control and cryogenic layer formation.

ACKNOWLEDGMENTS

The authors thank the NIF facility teams for their dedicated efforts during these experiments. This document was prepared as an account of work sponsored by an agency of the United States government. Neither the United States government nor Lawrence Livermore National Security, LLC, nor any of their employees makes any warranty, expressed or implied, or assumes any legal liability or responsibility for the accuracy, completeness, or usefulness of any information, apparatus, product, or process disclosed, or represents that its use would not infringe privately owned rights. Reference herein to any specific commercial product, process, or service by trade name, trademark, manufacturer, or otherwise does not necessarily constitute or imply its endorsement, recommendation, or favoring by the United States government or Lawrence Livermore National Security, LLC. The views and opinions of authors expressed herein do not necessarily state or reflect those of the United States government or Lawrence Livermore National Security, LLC, and shall not be used for advertising or product endorsement purposes. This work was performed under the auspices of the U.S.

Department of Energy by Lawrence Livermore National Laboratory under Contract Nos. DE-AC52-07NA27344 and LDRD 18-ERD-059 and 19-SI-002. This work was partially supported by Fusion Energy Sciences under Grant No. FWP 100182 and NNSA under Contract No. 89233119CNA000063. FST was supported by NNSA (LLNL-JRNL-817749).

DATA AVAILABILITY

The data that support the findings of this study are available from the corresponding author upon reasonable request.

REFERENCES

- ¹ A. Buffler, *Radiat. Phys. Chem.* **71**, 853 (2004).
- ² J. R. Srouf *et al.*, "Review of displacement damage effects in silicon devices," *IEEE Trans. Nucl. Sci.* **50**, 653 (2003).
- ³ Ch. J. Cerjan *et al.*, "Dynamic high energy density plasma environments at the National Ignition Facility for nuclear science research," *J. Phys. G: Nucl. Part. Phys.* **45**, 033003 (2018).
- ⁴ M. E. Gooden *et al.*, *Nucl. Data Sheets* **131**, 319 (2016).
- ⁵ Neutron Imaging: A Non-destructive Tool for Materials Testing Report of a Coordinated Research Project 2003–2006 September, IAEA-TECDOC-1604 (2008).
- ⁶ M. L. Spaeth *et al.*, *Fusion Sci. Technol.* **69**, 25 (2016).
- ⁷ J. Nuckolls, L. Wood, A. Thiessen, and G. Zimmerman, *Nature* **239**, 139 (1972).
- ⁸ J. D. Lindl, *Inertial Confinement Fusion: The Quest for Ignition and Energy Gain Using Indirect Drive* (Springer-Verlag, New York, 1998).
- ⁹ S. Atzeni and J. Meyer-ter Vehn, *The Physics of Inertial Fusion: Beam Plasma Interaction, Hydrodynamics, Hot Dense Matter*, International Series of Monographs on Physics (Clarendon Press, Oxford, 2004).
- ¹⁰ G. Ren *et al.*, *Phys. Rev. Lett.* **118**, 165001 (2017).
- ¹¹ H. Daido, M. Yamanaka, K. Mima, K. Nishihara, S. Nakai, Y. Kitagawa, E. Miura, C. Yamanaka, and A. Hasegawa, *Appl. Phys. Lett.* **51**, 2195 (1987).
- ¹² A. V. Bessab *et al.*, *Sov. Phys. JETP* **75**, 970 (1992).
- ¹³ Y. Abe *et al.*, *Appl. Phys. Lett.* **111**, 233506 (2017).
- ¹⁴ S. G. Garanin *et al.*, *J. Exp. Theor. Phys.* **128**, 650 (2019).
- ¹⁵ M. D. Rosen and J. H. Nuckolls, *Phys. Fluids* **22**, 1393 (1979).
- ¹⁶ S. W. Haan, M. C. Herrmann, T. R. Dittrich, A. J. Fetterman, M. M. Marinak, D. H. Munro, S. M. Pollaine, J. D. Salmonson, G. L. Strobel, and L. J. Suter, *Phys. Plasmas* **12**, 056316 (2005).
- ¹⁷ T. R. Boehly *et al.*, *Opt. Commun.* **133**, 495 (1997).
- ¹⁸ A. Nikroo and J. M. Pontelandolfo, *Fusion Technol.* **38**, 58 (2000).
- ¹⁹ M. Hohenberger *et al.*, *Rev. Sci. Instrum.* **85**, 11D501 (2014).
- ²⁰ W. Riedel, N. Meezan, D. Higginson, M. Hohenberger, J. Owen, and M. Cappelli, *High Energy Density Phys.* **37**, 100861 (2020).